J. Math. Biol. (2012) 64:1005–1020
DOI 10.1007/s00285-011-0436-2

Mathematical Biology

Joint effects of mitosis and intracellular delay on viral dynamics: two-parameter bifurcation analysis

Michael Y. Li · Hongying Shu

Received: 10 January 2011 / Revised: 15 May 2011 / Published online: 14 June 2011

Abstract To understand joint effects of logistic growth in target cells and intracellular delay on viral dynamics in vivo, we carry out two-parameter bifurcation analysis of an in-host model that describes infections of many viruses including HIV-I, HBV and HTLV-I. The bifurcation parameters are the mitosis rate r of the target cells and an intracellular delay τ in the incidence of viral infection. We describe the stability region of the chronic-infection equilibrium E^* in the two-dimensional (r, τ) parameter space, as well as the global Hopf bifurcation curves as each of τ and r varies. Our analysis shows that, while both τ and r can destabilize E^* and cause Hopf bifurcations, they do behave differently. The intracellular delay τ can cause Hopf bifurcations only when r is positive and sufficiently large, while r can cause Hopf bifurcations even when $\tau = 0$. Intracellular delay τ can cause stability switches in E^* while r does not.

Keywords Viral dynamics · In-host model · Intracellular delay · Stability switch · Periodic oscillations · Hopf bifurcation

Mathematics Subject Classification (2000) 92C50 · 34C23

M. Y. Li (✉) · H. Shu
Department of Mathematics, Harbin Institute of Technology, Harbin 150001, People's Republic of China
e-mail: mli@math.ualberta.ca

M. Y. Li · H. Shu
Department of Mathematical and Statistical Sciences, University of Alberta, Edmonton, AB T6G 2G1, Canada

1 Introduction

Intracellular delays and the target-cell dynamics such as mitosis are two key factors that play an important role in the viral dynamics. Mitosis in healthy or infected target-cell population are typically modelled by a logistic term (Perelson et al. 1993; Perelson and Nelson 1999; De Leenheer and Smith 2003; Nowak et al. 1996; Wang and Li 2006; Wang and Ellermeyer 2006). Intracellular delays have been incorporated into the incidence term in finite or distributed form (Culshaw and Ruan 2000; Herz et al. 1996; Li and Shu 2010a,b; Nelson et al. 2000; Nelson and Perelson 2002; Perelson et al. 1996; Wang et al. 2009). In Wang and Li (2006) and De Leenheer and Smith (2003), in-host viral models with a logistic growth term without intracellular delays are investigated, and it is shown that sustained oscillations can occur through Hopf bifurcation when the intrinsic growth rate increases. It is shown in (Culshaw and Ruan 2000; Wang et al. 2009), in in-host models with both a logistic growth term and intracellular delay, that Hopf bifurcations can occur when the intracellular delay increases. In Li and Shu (2010a,b), using in-host models with a general form of target-cell dynamics and general distributions for intracellular delays, it is shown that the occurrence of Hopf bifurcation in these models critically depends on the form of target-cell dynamics. More specifically, it is proved in Li and Shu (2010b) that, if the target-cell dynamics are such that no Hopf bifurcations occur when delays are absent, introducing intracellular delays in the model will not lead to Hopf bifurcations or periodic oscillations. In the light of these studies, for a full understanding of the joint effects of target-cell dynamics and intracellular delays on the viral dynamics, it is necessary to carry out two-parameter bifurcation analysis, where both r and τ are varied independently. This motivates our study in the present paper. We consider the following in-host model, which incorporates a logistic mitosis term for the uninfected target cells and a finite intracellular delay in the incidence term, as well as possibility of cell death during the delay phase,

$$\begin{aligned} x'(t) &= \lambda - d_1 x(t) + r x(t)\left[1 - \frac{x(t)}{x_{max}}\right] - \beta x(t) v(t), \\ y'(t) &= \beta e^{-s\tau} x\,(t-\tau)\, v\,(t-\tau) - d_2 y(t), \\ v'(t) &= k y(t) - d_3 v(t). \end{aligned} \tag{1}$$

In the model, $x(t)$, $y(t)$ and $v(t)$ denote the populations of uninfected target cells, infected target cells that produce virus, and free virus particles, respectively. Parameters d_1, d_2 and d_3 are turnover rates of the x, y and v compartments, respectively. Uninfected target cells are assumed to be produced at a constant rate λ. The mitosis of uninfected target cells is described by the logistic term $rx(t)(1 - x(t)/x_{max})$, where r is the intrinsic mitosis rate when $x(t)$ is small, and x_{max} is the maximum population of uninfected target cells maintained by homeostasis in the body. It is assumed that cells infected at time t will be activated and produce viral materials at time $t + \tau$. The number of actively infected target cells at time t is given by a delayed mass-action term

$$\beta e^{-s\tau} x\,(t-\tau)\, v\,(t-\tau).$$

Here constant s is the death rate of infected but not yet virus-producing cells, and $e^{-s\tau}$ describes the probability of infected target cells surviving the period of intracellular delay from $t-\tau$ to t. Constant k denotes the average number of virus particles each infected cell produces. All parameter values are assumed to be nonnegative with $d_1, d_2, d_3 > 0$.

System (1) can be used to model the infection dynamics of HIV-1, HBV and other virus (De Leenheer and Smith 2003; Nowak et al. 1996; Nowak and May 2000; Perelson et al. 1993; Perelson and Nelson 1999; Tuckwell and Wan 2004). It can also be considered as a model for the HTLV-I infection if $x(t)$, $y(t)$, and $v(t)$ are regarded as healthy, latently infected, and actively infected $CD4^+$ T cells (Nowak and Bangham 1996; Wang et al. 2002). For detailed description and derivation of the model, as well as the incorporation of intracellular delays, we refer the reader to our earlier work on this subject (Li and Shu 2010b).

Model (1) and related in-host models have been investigated under various possible assumptions including presence or absence of the intracellular delay, cell death of infected cells, and the logistic term. A key issue with intracellular delays is whether they cause sustained oscillations. This is typically investigated through Hopf bifurcations analysis. We summarize earlier results related to Hopf bifurcations in Table 1. For results summarized in Table 1, bifurcation studies are done by varying a single parameter, either the time delay τ or the mitosis rate r.

Our primary goal in the present paper is to carry out two-parameter bifurcation analysis of model (1) with bifurcation parameters r and τ, to gain a complete understanding of the impact of logistic growth term and intracellular delay, particularly the possibility of Hopf bifurcations and the global properties of the Hopf branches. Among our new discoveries are the following: (1) when only intracellular delay τ varies, Hopf bifurcation occurs if and only if the value of r satisfies $r \geq r_0$ for some $r_0 > 0$ (Theorems 3.4 and 3.5). This extends the result of Li and Shu (2010a,b) that, when $r = 0$, varying τ will not lead to Hopf bifurcations; (2) when cell death occur during the intracellular delay ($s > 0$) and for $r \geq r_0$, increasing intracellular delay τ can lead to stability switches in the chronic equilibrium E^* and the corresponding global Hopf branch is bounded. If $s = 0$, then stability switch does no occur; and (3) for all values of intracellular delay $\tau \geq 0$, increasing r will lead to Hopf bicurcations with forward unbounded Hopf branches, but no stability switches. Our results show

Table 1 Occurrence of Hopf Bifurcations in Model (1)

$\tau > 0$	$s > 0$	$r > 0$	Hopf bifurcations	References
N	N	N	N	Korobeinikov (2004)
N	N	Y	Y	Wang and Li (2006)
Y	N	N	N	Li and Shu (2010a,b)
Y	N	Y	Y	Wang et al. (2009)
Y	Y	N	N	Li and Shu (2010a); Herz et al. (1996); Li and Shu (2010b)

Y Yes, *N* No

that while both r and τ have a strong impact on the viral dynamics, the ways they exert their impact are quite different. Our theoretical results have significant implications when this type of models are used to explain experimental observations or to fit clinical data.

Our paper is organized as follows. In the next section, we derive the basic reproduction number R_0, and prove that, if $R_0 \leq 1$ then the infection-free equilibrium E_0 is globally stable; if $R_0 > 1$ then E_0 is unstable and a unique chronic-infection equilibrium E^* exists. In Sect. 3, we investigate the stability and bifurcation at E^* when $R_0 > 1$ by varying r and τ independently. And we also show numerical evidence to support our analytical results. A brief summary and discussions are given in Sect. 4.

2 Preliminaries

For $\tau > 0$, we denote by $\mathcal{C} = C([-\tau, 0], \mathbb{R})$ the Banach space of continuous real-valued functions on the interval $[-\tau, 0]$, with norm $\|\phi\| = \sup_{-\tau \leq \theta \leq 0} |\phi(\theta)|$ for $\phi \in \mathcal{C}$. The nonnegative cone of $\mathcal{C}$ is defined as $\mathcal{C}^+ = C([-\tau, 0], \mathbb{R}_+)$. Initial conditions for system (1) are chosen for $t = 0$ as

$$\varphi \in \mathcal{C}^+ \times \mathbb{R}_+ \times \mathcal{C}^+, \quad \varphi(0) > 0. \tag{2}$$

Let

$$f(x) = \lambda + (r - d_1)x - \frac{r}{x_{max}} x^2$$

and let $\overline{x}$ be the positive root of $f(x)$. The following result follows standard estimates.

Proposition 2.1 *All solutions of system* (1) *are positive and ultimately bounded in* $\mathcal{C} \times \mathbb{R} \times \mathcal{C}$. *Furthermore, the bounded regain*

$$\Gamma = \left\{ (x, y, v) \in \mathcal{C}^+ \times \mathbb{R}_+ \times \mathcal{C}^+ : \|x\| \leq \frac{\lambda}{d_1},\ \|x + y\| \leq \frac{\lambda}{\widetilde{\mu}},\ \|v\| \leq \frac{k\lambda}{d_3 \widetilde{\mu}} \right\},$$

where $\widetilde{\mu} = \min\{d_1, d_2\} > 0$, *is positively invariant with respect to model* (1) *and the model is well posed.*

Proof First, we prove that $x(t)$ is positive for all $t \geq 0$. Assuming the contrary and letting $t_1 > 0$ be the first time such that $x(t_1) = 0$, we have $x'(t_1) = \lambda > 0$, by the first equation of system (1). Hence $x(t) < 0$ for $t \in (t_1 - \epsilon, t_1)$, where $\epsilon > 0$ is sufficiently small. This contradicts $x(t) > 0$ for $t \in [0, t_1)$. It follows that $x(t) > 0$ for $t > 0$. Similarly, we can show the solutions $y(t)$, $v(t)$ of system (1) are positive for $t > 0$ under positive initial conditions. In fact, assuming the contrary and letting $t_2 > 0$ be the first time such that $v(t_2) = 0$, we have $v'(t_2) = ky(t_2)$, by the third equation of system (1). Solving $y(t)$ in the second equation of (1) we have

$$y(t_2) = \left[y(0) + \int_0^{t_2} \beta x(\theta - \tau)\, v(\theta - \tau)\, e^{-s\tau} e^{d_2 \theta} d\theta \right] e^{-d_2 t_2} > 0.$$

It follows that $v'(t_2) > 0$, and hence $v(t)$ is positive and

$$y(t) = \left[y(0) + \int_0^t \beta x\,(\theta - \tau)\, v\,(\theta - \tau)\, e^{-s\tau} e^{d_2\theta} d\theta \right] e^{-d_2 t} > 0.$$

From the first equation of (1) we obtain $x'(t) \leq \lambda - d_1 x(t)$, and thus $\limsup_{t\to\infty} x(t) \leq \frac{\lambda}{d_1}$. Adding the first two equations of (1) we get

$$\begin{aligned}(x(t) + y\,(t+\tau))' &= \lambda - d_1 x(t) - d_2 y(t+\tau) + \beta x(t) v(t) \left(e^{-s\tau} - 1\right) \\ &\leq \lambda - \widetilde{\mu}\,(x(t) + y(t+\tau)),\end{aligned}$$

where $\widetilde{\mu} = \min\{d_1, d_2\} > 0$. Thus $\limsup_{t\to\infty}(x(t) + y(t+\tau)) \leq \frac{\lambda}{\widetilde{\mu}}$. This relation and the third equation of (1) imply

$$v'(t) = k y(t) - d_3 v(t) \leq k\frac{\lambda}{\widetilde{\mu}} - d_3 v(t),$$

and $\limsup_{t\to\infty} v(t) \leq \frac{k\lambda}{d_3\widetilde{\mu}}$. Therefore, $x(t)$, $y(t)$ and $v(t)$ are ultimately bounded in $\mathcal{C} \times \mathbb{R} \times \mathcal{C}$. □

System (1) always has an infection-free equilibrium $E_0 = (\overline{x}, 0, 0)$. In addition to E_0, it is possible for the system to have a chronic-infection equilibrium $E_1 = (x^*, y^*, z^*)$ in the interior $\overset{\circ}{\Gamma}$ of Γ, with

$$x^* = \frac{d_2 d_3}{\beta k} e^{s\tau}, \quad y^* = \frac{d_3}{k} v^*, \quad v^* = \frac{f(x^*)}{\beta x^*}.$$

The dynamical outcomes of model (1) will be determined by the basic reproduction number

$$R_0 = \frac{\beta k \overline{x}}{d_2 d_3} e^{-s\tau}, \tag{3}$$

which descries the average number of productively-infected cells that arise from one infectious cell after it is introduced into a population of healthy target cells. We see that $0 < x^* < \overline{x}$ if and only if $R_0 > 1$, and this implies $v^* > 0$ since $f(x^*) > 0$ for $0 < x^* < \overline{x}$. The chronic equilibrium E^* exists in the interior of Γ if and only if $R_0 > 1$.

Using the Lyapunov functional $L : \mathcal{C} \times \mathbb{R} \times \mathcal{C} \to \mathbb{R}$

$$L(x_t, y(t), v_t) = e^{s\tau} y(t) + \frac{d_2 e^{s\tau}}{k} v_t(0) + \beta \int_{-\tau}^{0} x_t(\theta) v_t(\theta)\, d\theta$$

and a similar argument as in the proof of Theorem 3.2 in Li and Shu (2010a) (also see Li and Shu 2010b; Wang et al. 2009), we can prove the following stability result for the infection-free equilibrium E_0. The proof is omitted.

Proposition 2.2 *If $R_0 \le 1$. Then the infection-free equilibrium E_0 is globally asymptotically stable in Γ. If $R_0 > 1$, then E_0 is unstable.*

3 Stability of E^* and Hopf bifurcation

Assume that $R_0 > 1$ so that the chronic-infection equilibrium E^* exists. We investigate stability properties of E^*. Let $\tau_{max} = \frac{1}{s} \ln \frac{\beta k \bar{x}}{d_2 d_3}$ if $s > 0$, and $\tau_{max} = \infty$ if $s = 0$. Then $R_0 > 1$ implies that $0 \le \tau < \tau_{max}$. We investigate the dynamics of system (1) for $\tau \in [0, \tau_{max})$. Linearizing (1) around $E^* = (x^*, y^*, v^*)$ we obtain

$$\begin{aligned} x'(t) &= \left(r - d_1 - \beta v^* - \frac{2rx^*}{x_{max}}\right) x(t) - \beta x^* v(t), \\ y'(t) &= -d_2 y(t) + \beta v^* e^{-s\tau} x(t-\tau) + \beta x^* e^{-s\tau} v(t-\tau), \\ v'(t) &= k y(t) - d_3 v(t). \end{aligned} \tag{4}$$

The characteristic equation of (4) is

$$\xi^3 + a_2\xi^2 + a_1\xi + a_0 + (b_1\xi + b_0)\, e^{-\xi\tau} = 0, \tag{5}$$

whose coefficients are

$$a_2 = d_2 + d_3 + \frac{\lambda}{x^*} + \frac{rx^*}{x_{max}} > 0, \quad a_1 = d_2 d_3 + (d_2 + d_3)\left(\frac{\lambda}{x^*} + \frac{rx^*}{x_{max}}\right) > 0,$$
$$a_0 = d_2 d_3 \left(\frac{\lambda}{x^*} + \frac{rx^*}{x_{max}}\right) > 0, \quad b_1 = -d_2 d_3 < 0, \quad b_0 = -d_2 d_3 \left(d_1 + \frac{2rx^*}{x_{max}} - r\right).$$

We note that, if $s > 0$, then these coefficients are dependant on the delay τ, since x^* includes τ.

When $\tau = 0$, Eq. (5) becomes

$$\xi^3 + a_2\xi^2 + (a_1 + b_1)\,\xi + (a_0 + b_0) = 0.$$

Noticing that

$$a_2 > 0, \quad a_1 + b_1 = (d_2 + d_3)\left[\frac{\lambda}{x^*} + \frac{rx^*}{x_{max}}\right] > 0, \quad a_0 + b_0 = d_2 d_3 \beta v^* > 0,$$

and

$$a_2\left(a_1+b_1\right)-\left(a_0+b_0\right)=\left(d_2+d_3\right)\left[\frac{\lambda}{x^*}+\frac{rx^*}{x_{max}}\right]^2+\left(a^2+u^2\right)\left[\frac{\lambda}{x^*}+\frac{rx^*}{x_{max}}\right]$$
$$+d_2d_3\left[\frac{\lambda}{x^*}+d_1-r\left(1-\frac{3x^*}{x_{max}}\right)\right].$$

Routh–Hurwitz criterion implies that, when $\tau=0$, all roots of Eq. (5) have negative real parts if and only if the following condition holds.

$$a_2\left(a_1+b_1\right)-\left(a_0+b_0\right)>0 \quad \text{for } \tau=0. \tag{$\mathbf{H_0}$}$$

Proposition 3.1 *Assume $R_0>1$. Then, at $\tau=0$, the chronic-infection equilibrium E^* is locally asymptotically stable if and only if* ($\mathbf{H_0}$) *holds.*

Condition ($\mathbf{H_0}$) will be used to determine the stability region of E^* on the r-axis in the r–τ parameter space. At r values where ($\mathbf{H_0}$) holds, E^* is stable at $\tau=0$. We will let τ vary while holding r fixed and investigate possible bifurcations. For E^* to become unstable, characteristic roots have to cross the imaginary axis to the right when τ increases. Let $\xi=i\omega$ $(\omega>0)$ be a purely imaginary root of Eq. (5). Substituting it into (5) and separating the real and imaginary parts, we obtain

$$\begin{aligned}-\omega^3+a_1\omega&=b_0\sin\left(\omega\tau\right)-b_1\omega\cos\left(\omega\tau\right),\\ a_2\omega^2-a_0&=b_0\cos\left(\omega\tau\right)+b_1\omega\sin\left(\omega\tau\right).\end{aligned} \tag{6}$$

Squaring and adding both equations of (6) lead to

$$F\left(\omega,\tau\right):=\omega^6+p(\tau)\omega^4+q(\tau)\omega^2+l(\tau)=0, \tag{7}$$

where

$$\begin{aligned}p(\tau)&=a_2^2(\tau)-2a_1(\tau)=d_2^2+d_3^2+\left(\frac{\lambda}{x^*}+\frac{rx^*}{x_{max}}\right)^2>0,\\ q(\tau)&=a_1^2(\tau)-2a_0(\tau)a_1(\tau)-b_1^2=\left(d_2^2+d_3^2\right)\left(\frac{\lambda}{x^*}+\frac{rx^*}{x_{max}}\right)>0,\\ l(\tau)&=a_0^2-b_0^2=d_2^2u^2\beta v^*\left[\frac{\lambda}{x^*}+d_1-r\left(1-\frac{3x^*}{x_{max}}\right)\right].\end{aligned} \tag{8}$$

Then a root $i\omega$ $(\omega>0)$ of Eq. (5) satisfies $F(\omega,\tau)=0$. Since $p(\tau)>0, q(\tau)>0$ for all $\tau\geq 0$, we know that $F(\omega,\tau)=0$ have positive roots if and only if $l(\tau)<0$, or equivalently, if and only if

$$\frac{\lambda}{x^*}+d_1-r\left(1-\frac{3x^*}{x_{max}}\right)<0. \tag{$\mathbf{H_1}$}$$

If ($\mathbf{H_1}$) holds, then $F(0,\tau) = l(\tau) < 0$. Continuity of $F(\omega,\tau)$ implies that $F(\omega,\tau) = 0$ has a solution $\omega > 0$ for each $\tau > 0$, since $\lim_{\omega\to+\infty} F(\omega,\tau) = +\infty$. As $\frac{\partial F(\omega,\tau)}{\partial\omega} = 6\omega^5 + 4p(\tau)\omega^3 + 2q(\tau)\omega > 0$ for $\omega > 0$, the Implicit Function Theorem implies that there exists a unique C^1 function $\omega = \omega(\tau) > 0$ such that $F(\omega(\tau),\tau) = 0$ for $\tau > 0$. We thus obtained the following result.

Lemma 3.2 *If ($\mathbf{H_1}$) holds, then $F(\omega,\tau) = 0$ has a unique positive root $\omega = \omega(\tau)$, for $\tau > 0$.*

Let $\omega = \omega(\tau) > 0$ be the unique positive root of $F(\omega(\tau),\tau) = 0$. For $i\omega(\tau)$ to be a solution to the characteristic Eq. (5), $\omega(\tau)$ needs to satisfy the system

$$\begin{aligned} \sin\omega(\tau)\tau &= \frac{(a_2b_1 - b_0)\omega(\tau)^3 + (a_1b_0 - a_0b_1)\,\omega(\tau)}{b_1^2\omega(\tau)^2 + b_0^2} := f_1(\tau), \\ \cos\omega(\tau)\tau &= \frac{b_1\omega(\tau)^4 + (a_2b_0 - a_1b_1)\omega(\tau)^2 - a_0b_0}{b_1^2\omega(\tau)^2 + b_0^2} := f_2(\tau). \end{aligned} \tag{9}$$

Define $\theta(\tau) \in (-\pi,\pi]$ as

$$\theta(\tau) = \arccos\left(f_2(\tau)\right)\mathrm{Sign}(f_1(\tau)).$$

Following Beretta and Kuang (2002), we set

$$S_n(\tau) = \tau - \frac{\theta(\tau) + 2n\pi}{\omega(\tau)}, \quad \tau \in (0,\tau_{max}) \quad \text{with } n \in \mathbb{N}. \tag{10}$$

Then $\pm i\omega(\tau^*)$ are purely imaginary roots of (5) if and only if τ^* is a zero of function S_n for some $n \in \mathbb{N}$.

Proposition 3.3 *Assume that the function $S_n(\tau)$ has a positive root $\tau^* \in (0,\tau_{max})$, for some $n \in \mathbb{N}$, then a pair of simple purely imaginary roots $\pm i\omega(\tau^*)$ of (5) exist at $\tau = \tau^*$, and*

$$\mathrm{Sign}\left\{\frac{dRe(\xi)}{d\tau}\bigg|_{\xi=i\omega(\tau^*)}\right\} = \mathrm{Sign}\left\{\frac{dS_n(\tau)}{d\tau}\bigg|_{\tau=\tau^*}\right\}. \tag{11}$$

Furthermore, the pair of simple purely imaginary roots $\pm i\omega$ cross the imaginary axis to the right at $\tau = \tau^*$ if $S_n'(\tau^*) > 0$.

Proof Relation (11) follows from the following equality in Beretta and Kuang (2002)

$$\mathrm{Sign}\left\{\frac{d\mathrm{Re}(\xi)}{d\tau}|_{\xi=i\omega(\tau^*)}\right\} = \mathrm{Sign}\left\{\frac{\partial F}{\partial\omega}\left(\omega(\tau^*),\tau^*\right)\right\} \times \mathrm{Sign}\left\{\frac{dS_n(\tau)}{d\tau}|_{\tau=\tau^*}\right\}.$$

and the fact that $\frac{\partial F}{\partial\omega}(\omega(\tau^*),\tau^*) > 0$. □

The following properties of $S_n(\tau)$ can be verified using (10).

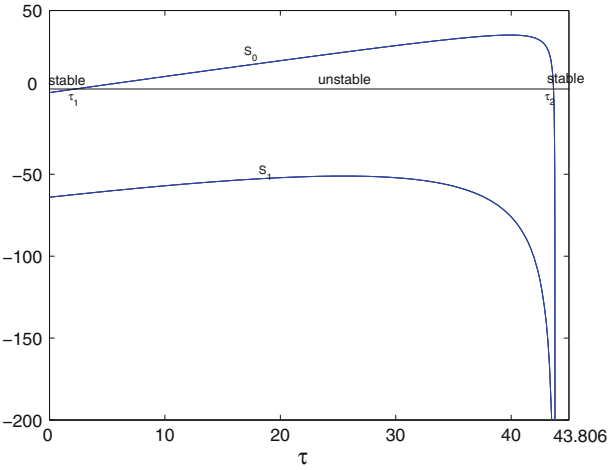

Fig. 1 Graph of functions S_0 and S_1 for $\tau \in (0, \tilde{\tau})$ with parameters given in (13)

(a) $S_n(\tau) \geq S_{n+1}(\tau)$, $n \in \mathbb{N}$. Therefore, if S_0 has no zeros in $(0, \tau_{max})$, nor does S_n, $n > 0$.

(b) Let

$$\tilde{\tau} = \sup\{\tau \in (0, \tau_{\max}) \mid (\mathbf{H_1}) \text{ holds}\}.$$

Then $l(\tilde{\tau}) = 0$, and thus $\omega(\tau) \to 0$ while $\sin\theta(\tau) \to 0$ and $\cos\theta(\tau) \to -1$, as $\tau \to \tilde{\tau}^-$. As a consequence, $\theta(\tau) \to \pi$ and $S_n(\tau) \to -\infty$, as $\tau \to \tilde{\tau}^-$.

(c) When $\tau = 0$, if $r > 0$ satisfies ($\mathbf{H_0}$), then E^* is asymptotically stable and the first pair of eigenvalues can only cross the imaginary axis at $\tau > 0$. Therefore $S_0(0) < 0$ in this case. Similarly, at r values that ($\mathbf{H_0}$) does not hold, $S_0(0) \geq 0$.

From properties (b) and (c) we know that if $S_0(0) < 0$ and $S_0(\tau)$ has a positive zero, then $S_0(\tau)$ necessarily has at least two positive zeros in $(0, \tilde{\tau})$. As we show in Fig. 1, when $S_0(0) < 0$, $S_0(\tau)$ has two positive zeros $0 < \tau_1 < \tau_2 < \tau_{max}$, with $S_0'(\tau_1) > 0$ and $S_0'(\tau_2) < 0$. A pair of complex conjugate eigenvalues cross the imaginary axis to the right at $\tau = \tau_1$, remain to the left for $\tau_1 < \tau < \tau_2$, and cross back to the right at $\tau = \tau_2$. Accordingly, E^* remains stable for $\tau \in (0, \tau_1)$, loses its stability for $\tau \in (\tau_1, \tau_2)$, and regains its stability for $\tau > \tau_2$. This is the so-called stability switch phenomenon. Accompanying the stability switches, a branch of stable periodic solutions exists for $\tau \in (\tau_1, \tau_2)$, as depicted in Fig. 2. In Fig. 3, we show that solutions converge to the stable E^* for $\tau < \tau_1$, and that solutions converge to a stable periodic solutions for $\tau \in (\tau_1, \tau_2)$.

While stability switches produced by time delays have been discussed in Beretta and Kuang (2002) and other studies in the literature, properties of the global Hopf bifurcation branch that accompanies the stability switch have not received much attention. We refer interested readers to a recent work Li and Shu (2010) where stability switches are show to be able to produce coexistence of multiple stable periodic solutions in delayed systems. We note that our discussion of stability switches is slightly different from that

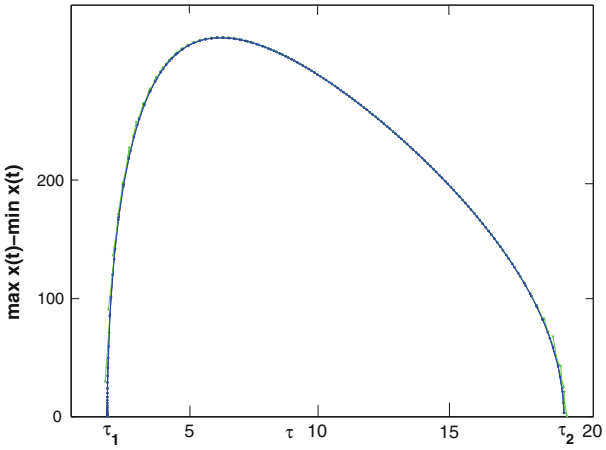

Fig. 2 Global Hopf bifurcation branch is computed using Matlab when we vary τ and keep $r = 0.03$. Equilibrium goes through stability switches at $\tau = \tau_1 \approx 1.87$ and $\tau = \tau_2 \approx 18.04$. A global Hopf brach of stable periodic solutions exists for $\tau \in (\tau_1, \tau_2)$

in Beretta and Kuang (2002) in that we choose $\theta(\tau) \in (-\pi, \pi]$ while $\theta(\tau) \in (0, 2\pi]$ in Beretta and Kuang (2002). Our definition has allowed us to discover the possibility that $S_0(0)$ can be positive, and as a consequence, $S_0(\tau)$ has exactly one positive root τ_2. This is described in Case (iii) of Theorem 3.5, and it corresponds to the situation that E^* is already unstable when $\tau = 0$ due to the presence of sufficiently large mitosis, and a periodic solution exists due to the Hopf bifurcation created by the mitosis rate r. When we increase τ while holding r at this value, we see that the Hopf branch extends for $\tau > 0$ and terminates at τ_2; stability switch does not occur in such a case, see Fig. 2. We also note that switches caused by $S_1(\tau)$ having multiple positive zeroes are possible theoretically but were not observed in our numerical experiments. Such switches (caused by S_1) will not affect the stability of E^*, but may lead to additional Hopf branches.

In the next result, we show that varying the delay τ will not always lead to instability of E^*; the rate r of mitosis needs to be sufficiently large for delay-caused instability to occur.

Theorem 3.4 *There exists $r_0 > 0$ such that, when $0 \le r < r_0$, the chronic-infection equilibrium E^* is asymptotically stable for all $0 \le \tau < \tau_{max}$.*

Proof Since $x^*(\tau) < \bar{x}$ for $\tau \in (0, \tau_{max})$, there exists $r_0 > 0$ such that when $0 \le r < r_0$,

$$\frac{\lambda}{x^*(\tau)} + d_1 - r\left(1 - \frac{3x^*(\tau)}{x_{max}}\right) > 0 \quad \text{for } \tau \in (0, \tau_{max})\,. \tag{12}$$

Therefore, condition ($\mathbf{H_1}$) is violated, and thus $F(\omega, \tau) = 0$ has no positive roots ω. This implies that no characteristic roots cross the imaginary axis for $\tau \in (0, \tau_{max})$. When $\tau = 0$, condition (12) agrees with condition ($\mathbf{H_0}$). We thus conclude that

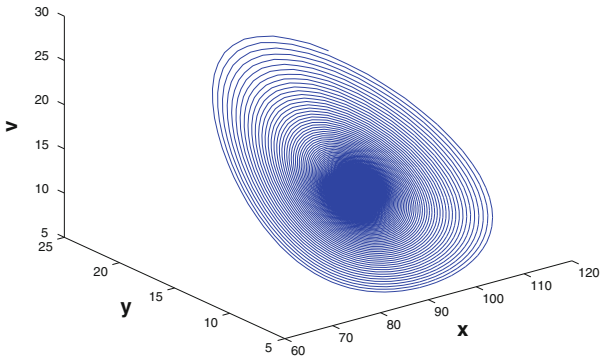

(a) local asymptotic stability of E^* with $\tau = 0.01 < \tau_1$.

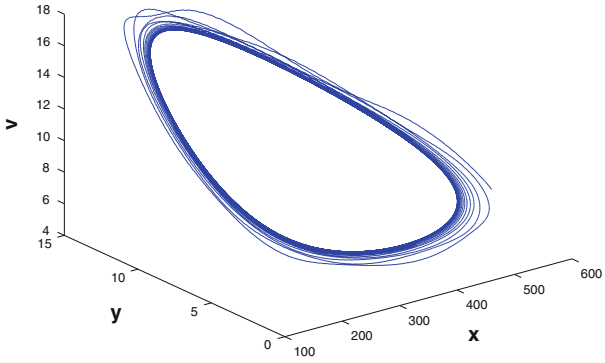

(b) Solutions converge to a stable periodic solution with $\tau = 40 \in (\tau_1, \tau_2)$.

Fig. 3 Simulation of solutions to (4) for different values of r and τ. Parameter values for the simulations are given in (13)

E^* is asymptotically stable when $\tau = 0$ and remains asymptotically stable for $\tau \in (0, \tau_{max})$. □

We remark that Theorem 3.4 holds for both $s > 0$ and for $s = 0$, and in the latter case, $\tau_{max} = +\infty$. It was shown in Li and Shu (2010b) that, if $r = 0$, then E^* remains asymptotically stable for all delays $\tau > 0$. Theorem 3.4 further generalizes this result of Li and Shu (2010b) in that it establishes an open interval for the mitosis rate, $0 < r < r_0$, for which the time delays will not destabilize E^*. Theorem 3.4 reveals the importance of mitosis in the viral infection process; time delays can destabilize E^* only if the mitosis rate is positive and sufficiently large.

Theorem 3.5 *Assume that $R_0 > 1$. Then the following conclusions hold.*

(i) *For all r values such that ($\mathbf{H_0}$) holds and that $S_0(\tau)$ has no positive zeros, no Hopf bifurcation occurs and the equilibrium E^* remains asymptotically stable for all $0 \le \tau < \tau_{max}$,*

(ii) *For all r values such that ($\mathbf{H_0}$) holds and that $S_n(\tau)$, $n \ge 0$, have positive simple zeros, $\tau_1 < \tau_2 < \cdots < \tau_m$, system (1) undergoes a Hopf bifurcation at the equilibrium E^* when $\tau = \tau_i, i = 1, m$. The Hopf bifurcation is supercritical at $\tau = \tau_1$ and subcritical at $\tau = \tau_m$. Furthermore, E^* goes through stability switches: E^* is asymptotically stable for $\tau \in [0, \tau_1) \cup (\tau_m, \tau_{max})$, and unstable when $\tau \in (\tau_1, \tau_m)$.*

(iii) *For all r values such that ($\mathbf{H_0}$) does not hold, E^* is unstable when $\tau = 0$. Let $\tau_1 < \tau_2 < \cdots < \tau_m$ be the positive roots of $S_n(\tau)$, $n \ge 0$. Then the equilibrium E^* remains unstable for $\tau \in [0, \tau_m)$, and asymptotically stable for $\tau \in (\tau_m, \tau_{max})$. A subcritical Hopf bifurcation occurs at $\tau = \tau_m$. As τ increases, a global Hopf branch starts at $\tau = 0$ continues and terminates at $\tau = \tau_m$.*

In Fig. 4a, we show the stability region of E^* in the r–τ parameter space, for the following set of parameter values:

$$\lambda = 0.1,\ d = 0.02,\ x_{max} = 1500,\ \beta = 0.0027,$$
$$s = 0.03,\ a = 0.3,\ k = 3,\ u = 2.4. \tag{13}$$

Corresponding to the three cases in the conclusions of Theorem 3.5, the horizontal r-axis is divided into three intervals:

(i) for all $r \in (0,\ 0.027)$, the equilibrium E^* remains asymptotically stable for all values of τ and no Hopf bifurcations occurs when τ varies.

(ii) for $r \in (0.027,\ 0.09)$ [see the blow-up picture in Fig. 4b], $S_0(\tau)$ has two positive roots $\tau_1(r)$ and $\tau_2(r)$. Equilibrium E^* undergoes stability switches as τ increases: first loses stability at $\tau_1(r)$ and then regains the stability at $\tau_2(r)$. When τ increases, a global Hopf branch exists and connects $\tau_1(r)$ and $\tau_2(r)$ as is shown in Fig. 2.

(iii) for $r \in (0.09,\ 0.1)$, the equilibrium E^* is unstable when $\tau = 0$, and $S_0(\tau)$ has only one positive root $\tau_2(r)$. A stable periodic solution exists for $\tau = 0$ and continues to exist for $\tau \in (0, \tau_2(r))$. At $\tau = \tau_2(r)$, the Hopf branch terminates, and E^* becomes stable.

The bifurcation analysis at E^* as we vary r is similar to that for the case when τ is varied, only is much simpler. In the following, we fix $\tau \in [0, \tau_{max})$ and let r vary in $[0, \infty)$. We have established in Theorem 3.4 that E^* is asymptotically stable when $r = 0$. When r increases from 0, we investigate whether and when eigenvalues cross the imaginary axis. This beings us back to Eq. (7), and we regard r as a variable and τ fixed,

$$F(\omega, r) = \omega^6 + p(r)\omega^4 + q(r)\omega^2 + l(r) = 0, \tag{14}$$

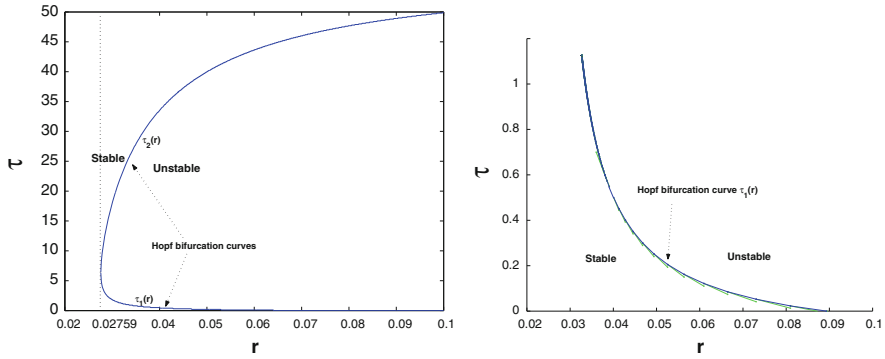

(a) Region of stability of E^* and Hopf bifurcations curves in the r-τ parameter space.

(b) Amplification of the lower branch $\tau_1(r)$ of the Hopf bifurcation curve in (a).

Fig. 4 Stability region of E^* and Hopf bifurcation curves in the r–τ parameter space. Other parameter values are as given in (13)

where, as in (8), we know $p(r) > 0, q(r) > 0$, and

$$l(r) = d_2^2 u^2 \beta v^* \left[\frac{\lambda}{x^*} + d_1 - r\left(1 - \frac{3x^*}{x_{max}}\right)\right].$$

Equation $F(\omega, r) = 0$ has a unique positive solution $\omega = \omega(r)$ if and only if $l(r) < 0$. When $R_0 > 1$, we know that $0 < x^* < \bar{x}$ and $v^* = f(x^*) > 0$. Therefore, the sign of $l(r)$ is determined by the linear expression of r,

$$\frac{\lambda}{x^*} + d_1 - r\left(1 - \frac{3x^*}{x_{max}}\right).$$

Since $l(0) > 0$, we know whether $F(\omega, r) = 0$ has a positive root depends on the sign of $1 - 3x^*/x_{max}$. Using $x^* = \frac{d_2 d_3}{\beta k} e^{s\tau}$ we obtain the following result on the bifurcation at E^* when r varies.

Theorem 3.6 *Assume that $R_0 > 1$. Then the following holds.*

(i) *If $x_{max} \leq \frac{3d_2 d_3 e^{s\tau}}{\beta k}$, then $F(\omega, r) = 0$ has no positive roots and E^* remains asymptotically stable for all $r \in [0, \infty)$.*
(ii) *If $x_{max} > \frac{3d_2 d_3 e^{s\tau}}{\beta k}$, then there exists a unique $\bar{r} > 0$ such that $F(\omega, \bar{r}) = 0$. The chronic-infection equilibrium E^* is asymptotically stable if $0 \leq r < \bar{r}$ and unstable if $r > \bar{r}$. A Hopf bifurcation occurs at $r = \bar{r}$.*

In Fig. 4a, if we fix $\tau \in (0, \tau_{max})$ and let (r, τ) increase horizontally in the r direction, we see that E^* loses its stability at the Hopf bifurcation curve $\tau_1(r)$ or $\tau_2(r)$, and remains unstable. A forward supercritical Hopf bifurcation occurs at $\tau_1(r)$ or $\tau_2(r)$. A global Hopf bifurcation branch is computed using Matlab and shown in Fig. 5 as r varies and τ fixed at $\tau = 15$.

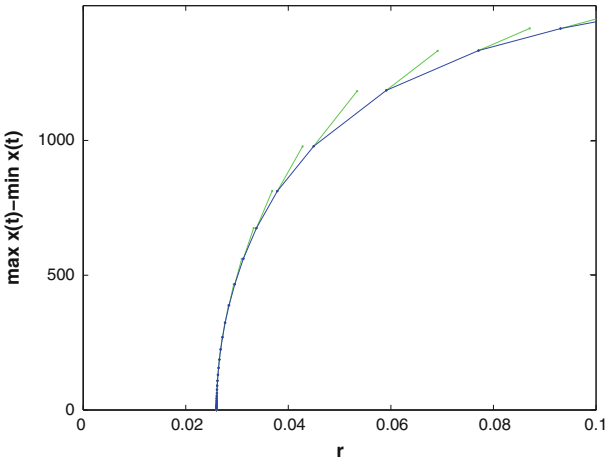

Fig. 5 Global Hopf bifurcation branch as we vary r while keeping $\tau = 15$. No stability switches occur

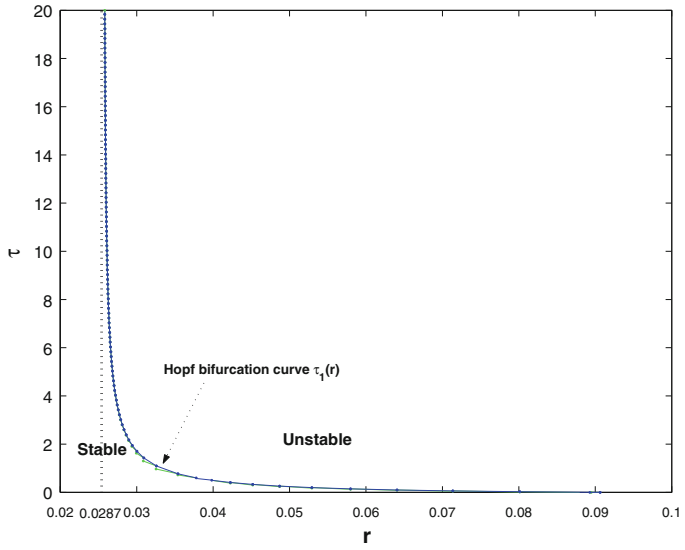

Fig. 6 Region of stability of E^* and a Hopf bifurcations curves in the r–τ parameter space when $s = 0$. All other parameter values are given in (13). We see that no stability switches occur in either r or τ direction

The preceding analysis also holds for the case $s = 0$. The stability region of E^* in the r–τ plane is shown in Fig. 6, for $s = 0$ and other parameters as in (13). We see that the shape of the Hopf bifurcation curve is different for the case $s = 0$, in comparison to the case $s > 0$ in Fig. 4a, and has only a single branch. Accordingly, no stability switches will occur in either direction, and periodic solutions will persists for large values of τ and r.

4 Summary and discussion

In this paper, using a standard mathematical model, we have investigated the joint effects of mitosis rate r of the target cells and an intracellular delay τ in the viral replication inside a target cell on the dynamics of viral infections in vivo. When varied independently, each of these two factors are known in the literature to lead to instability of the chronic-infection equilibrium E^* and produces stable periodic oscillations through Hopf bifurcation. We have carried out bifurcation analysis at E^* allowing both r and τ to change independently, and our results have established, through both analytical and numerical analysis, the global bifurcation diagram in the two dimensional r–τ parameter space (see Fig. 3). Among the new understandings are the following.

1. While r and τ can both lead to instability and oscillations, the fashion in which they exert their influence is different. Increasing the mitosis rate r can lead to Hopf bifurcation at E^* even in the absence of the intracellular delay; while increasing the intracellular delay τ will not lead to Hopf bifurcation or instability in the absence of mitosis. In fact, τ produces Hopf bifurcation only when the mitosis rate r is sufficiently large. Our results suggest that target-cell dynamics as represented in the model by mitosis play a more essential role compared to intracellular delays.
2. Varying the mitosis rate r produces a forward supercritical Hopf bifurcation with a unbounded global Hopf branch when r is large (see Fig. 5); while varying the intracellular delay τ can produce stability switches, with bounded global Hopf branches (see Fig. 2). The occurrence of stability switch is biologically significant, since the range of delays over which oscillations occur is finite and dependent on the parameter values. When medical interventions are applied to vary values of parameters other than τ, the range of delays for oscillations may change and lead to occurrence or disappearance of oscillations, even when the delay τ remains constant.

These new understandings on the role played by the mitosis and intracellular delay can help us better interpret experimental or clinical observations. Our conclusions are based on relatively simple models. We believe that further studies are needed to investigate important roles played by target-cell dynamics, intracellular delays in other stages of the viral infection process, and the roles played by immune reactions against viral infections and latent viral reservoirs (Rong and Perelson 2009).

Acknowledgments The research supported in part by grants from the Natural Science and Engineering Research Council (NSERC) and Canada Foundation for Innovation (CFI). H. Shu acknowledges the financial support of a scholarship from the China Scholarship Council while visiting the University of Alberta. Both authors acknowledge the support from the Mathematics of Information Technology and Complex Systems (MITACS).

References

Beretta E, Kuang Y (2002) Geometric stability switch criteria in delay differential systems with delay dependent parameters. SIAM J Math Anal 33:1144–1165

Culshaw RV, Ruan SG (2000) A delay-differential equation model of HIV infection of $CD4^+$ T-cells. Math Biosci 165:27–39

De Leenheer P, Smith HL (2003) Virus dynamics: a global analysis. SIAM J Appl Math 63:1313–1327
Herz V, Bonhoeffer S, Anderson R, May R, Nowak M (1996) Viral dynamics in vivo: limitations on estimates of intracellular delay and virus decay. Proc Natl Acad Sci USA 93:7247–7251
Korobeinikov A (2004) Global properties of basic virus dynamics models. Bull Math Biol 66:879–883
Li MY, Shu H (2010) Global dynamics of an in-host viral model with intracellular delay. Bull Math Biol 72:1429–1505
Li MY, Shu H (2010) Impact of intracellular delays and target-cell dynamics on in vivo viral infections. SIAM J Appl Math 70:2434–2448
Li MY, Shu H (2010) Multiple stable periodic oscillations in a mathematical model of CTL response to HTLV-I infection, Bull Math Biol (published online)
Nelson PW, Murray J, Perelson A (2000) A model of HIV-1 pathogenesis that includes an intracellular delay. Math Biosci 163:201–215
Nelson PW, Perelson AS (2002) Mathematical analysis of delay differential equation models of HIV-1 infection. Math Biosci 179:73–94
Nowak MA, Bangham CRM (1996) Population dynamics of immune responses to persistent viruses. Science 272:74–79
Nowak MA, Bonhoeffer S, Hill AM, Boehme R, Thomas HC (1996) Viral dynamics in hepatitis B virus infection. Proc Natl Acad Sci USA 93:4398–4402
Nowak MA, May RM (2000) Virus dynamics. Cambridge University Press, Cambridge
Perelson AS, Kirschner DE, de Boer R (1993) Dynamics of HIV infection of $CD4^+$ T cells. Math Biosci 114:81–125
Perelson AS, Nelson PW (1999) Mathematical analysis of HIV-I dynamics in vivo. SIAM Rev 41:3–44
Perelson AS, Neumann AU, Markowitz M et al (1996) HIV-1 dynamics in vivo: virion clearance rate, infected cell life-span, and viral generation time. Science 271:1582–1586
Rong L, Perelson AS (2009) Modeling HIV persistence, the latent reservoir, and viral blips. J Theor Biol 260:308–331
Tuckwell HC, Wan FYM (2004) On the behavior of solutions in viral dynamical models. Biosystems 73:157–161
Wang L, Ellermeyer S (2006) HIV infection and $CD4^+$ T cell dynamics. Discret Contin Dyn Syst B6:1417–1430
Wang L, Li MY (2006) Mathematical analysis of the global dynamics of a model for HIV infection of $CD4^+$ T cells. Math Biosci 200:44–57
Wang L, Li MY, Kirschner D (2002) Mathematical analysis of the global dynamics of a model for HTLV-I infection and ATL progression. Math Biosci 179:207–217
Wang Y, Zhou YC, Wu JH, Heffernan J (2009) Oscillatory viral dynamics in a delayed HIV pathogenesis model. Math Biosci 219:104–112